Fabrication of milk protein-based electrospun nanofibers

by

Wangyi We

B.S., Kansas State University, 2019

A REPORT

submitted in partial fulfillment of the requirements for the degree

MASTER OF SCIENCE

Food Science

KANSAS STATE UNIVERSITY
Manhattan, Kansas

2022

Approved by:

Major Professor
Jayendra K. Amamcharla

Copyright

Abstract

The electrospinning technique has been applied to various biopolymers for nanofiber fabrication. In this report, dairy protein based electrospun nanofibers have been fabricated for its potential application as edible coating material. Whey protein and casein are the two major proteins in milk. It has been known that electrospinning of dairy proteins (Whey and Casein) is a challenge due the complex secondary and tertiary structure, and weak internal interactions of dairy proteins. Thus, the first step of the research was about exploration of process parameters during electrospinning of dairy protein. Since the addition Polyvinyl alcohol (PVA) to Whey protein isolate (WPI) solution has an effect on the spinnability, different ratios of WPI and PVA were evaluated. The WPI: PVA mixture and fibers were evaluated in terms of viscosity, conductivity, surface tension, and SEM (scanning electron microscopy) of the nanofiber. In addition, heat denatured whey proteins has been denatured for 2 hours, and the pH of the WPI solution were adjusted to 2 because whey protein exhibits a better spinnability in acid conditions (Vega‐Lugo, 2012). Viscosity and surface tension were increased with the addition of PVA while conductivity was inversely decreased. High concentration of WPI and PVA (6%WPI with 5% and 6% PVA) solutions were not spinnable due to the high viscosity induced rapid solidification at the tip of the syringe. According to the SEM images, fine, beads-free nanofibers were generated with higher PVA concentrations while there were no significant differences among the nanofibers with various WPI concentrations.

The effect of PVA on electrospinning of whey protein has been investigated, another dairy protein, casein micelle was also used for fabricating electrospun nanofiber. The effects of MCC (micelle casein concentrate) and PVA (polyvinyl alcohol) blend composition on the spinnability of MCC/PVA solution and the morphology of electrospun nanofiber have been investigated. A

blend of MCC and PVA was prepared at different concentrations (MCC: 8, 10, 12, 14% wt, PVA: 0, 1, 2, 3% wt.). As expected, the apparent viscosity of MCC and PVA blends increased significantly (P-value$\leqslant$0.05) with an increase in MCC and PVA concentration which increased the diameter of nanofiber, while there was only a slight increase in surface tension. The collected nanofibers were characterized using Fourier transform infrared spectroscopy and scanning electron microscopy. From the SEM images, the MCC: PVA blend exhibited nanofiber quality improvement and the ability to form orientationally nonwovens nanofibers which can be collected as edible film. Addition of both MCC and PVA contributes to the spinnability of blend. However, MCC alone did not possess the effect of increasing spinnability while PVA itself can eliminate formation of beads. To form fine, smooth, uniformly sized nanofiber, the blend requires at least 2% PVA.

Table of Contents

Table of Contents v
List of Figures vi
List of Tables vii
Acknowledgements viii
Chapter1 Introduction 1
Chapter2 Literature Review 5
Edible Film 5
Principle and Process of Electrospinning 8
Overview of Dairy Ingredients 11
PVA (Polyvinyl alcohol) 15
Chapter3 Methodology 16
Experimental design 16
Phase I 17
Phase II 19
Chapter4 Results & Discussion 22
Phase I 22
Phase II 31
Chapter5 Conclusion 38
References 40
Appendix A 45

List of Figures

Fig. 2-1 Schematic illustration of the basic setup for electrospinning system. (Nieuwland et al., 2013). 8
Fig. 4-1 Electrospinning result of 10% MCC with 0.2% SHMP. 26
Fig. 4-2 Scanning electron micrographs of WPI-PVA electrospun fibers. A(left) 6% WPI /1%PVA, B(right), 8% WPI/1% PVA 26
Fig. 4-3 The SEM image of electrospun fiber of mixture of WPI-PVA solutions under pH=2. The row represented of PVA concentration (4,5,6% wt) and the column represented the WPI concentration at resolution 5μm. The image h and I represent that the 6% WPI with 5%PVA 30
Fig. 4-4 Scanning electron microscope of MCC-PVA nanofiber. The SEM image of electrospun nanofiber of the blend of MCC-PVA solutions at different concentrations. The column represents the PVA concentration (1, 2, 3,% wt) and the row represents the MCC concentration 35
Fig. 4-5 FTIR spectrum of electrospun nanofiber film of MCC/PVA with ratio 1% PVA+ 8%, 10%, 12% MCC. 37

List of Tables

Table 4-1 Feasibility and morphology of electrospinning product from modified protein solutions. 24
Table 4-2 Viscosity(mPa·s) change of pure MCC solution with addition SHMP..... 24
Table 4-3 Conductivity(uS/cm) of MCC/SHMP blends..... 25
Table 4-4 Solution properties and electrospinning feasibility of WPI/PVA solutions..... 25
Table 4-5 Physical characteristics of WPI-PVA solution..... 28
Table 4-6 Physical characteristics of MCC-PVA solution 33
Table 4-7 The diameter of nanofiber at different concentrations of MCC/PVA..... 36

Acknowledgements

I thank Dr. Jayendra Amamcharla (College of Agriculture/Department of Food Science) for his financial support and guidance for my master's research. I am thankful to my families and my colleagues in my group for their support and happiness they brought to me during my studying life.

Chapter1 Introduction

The use of edible films and coatings was proposed as packaging material to ensure food security by providing sealable protection to reduce physicochemical contaminations and extend the shelf-life of foods. The electrospun nanofibers were considered as a novel material for edible film packaging due to their structural and functional advantages. Utilizing the electrospun nanofiber as packaging materials may satisfy consumer demand of active packaging with an aim to improve safety and nutritional value. For packaging purposes, electrospun nanofibers have been covalently or non-covalently functionalized for loading commercial dry ingredients or bioactive compounds as active food packaging (Zhang et al, 2020).

Electrospinning is a process to create solid nanofiber by continuously stretching an electrically charged jet. It is a novel technique of nanofiber formation which counteracts the surface tension of the solution by utilizing electrostatic repulsive force to achieve the purpose of rearranging the polymer and removing extra solvents. In the food industry, electrospinning has been applied to the preservation and compound carrier through encapsulation and incorporation of bioactive compounds into nanofibers. In addition, electrospinning involves no heat, which is a key factor for minimizing the heat induced changes on structure and functional properties of sensitive compounds. Based on these features, fabrication of functional materials by electrospinning can be used for active packaging, edible film preparation, and stabilization of nutraceuticals etc (insert reference). A successful electrospun nanofiber fabrication involves a series of parameters, such as spinning solution characteristics, ambient conditions, and processing parameters (Wen et al, 2017). The electrospinning technique involves a high voltage applied on the viscous solution, and the positively charged solution is pumped dropwise through

the syringe to form a Taylor cone by the electric field. A continuous, stable jet is required for the edible film after the formation of the Taylor cone which is eminently related to the presence of chain entanglement and elongational viscosity (Shenoy et al., 2005). Since the core requirement of a successful electrospinning process is whether the repulsive force of the electric field can overcome surface tension or not, intensifying the strength of the electric field can directly increase the success rate of dairy protein nanofiber fabrication. On the other hand, reduction of surface tension or remaining constant while strengthening electrical force can indirectly contribute to the electrospinning process as well.

Nanofibers are fibers within about 50 to 500 nanometers in diameter depending on the type of polymers used, such as polysaccharides, gelatin, cellulose, and protein (Vasita & Katti, 2006). Furthermore, the nanofibers can also be generated with synthetic polymers including PEO (polyethylene glycol), PVA (polyvinyl alcohol), PLA (polylactic acid), PCL (polycaprolactone), PEVA (polyethylene-co-vinylacetate), etc. Electrospun nanofiber from dairy protein has been extensively studied due to its biodegradability and biocompatibility, especially cooperating with other polymers for edible film manufacturing. For instance, the corporation between guar gum and whey protein, or cooperation between PEO and whey protein provides the idea of overcoming the challenges of dairy protein electrospinning (Vega-Lugo, & Lim, 2012). It has been proved that dissolving biopolymers such as proteins into organic solvents such as 2,2,2-trifluoroethanol (TFE) can successfully produce electrospun fiber (Matthews et al, 2002). However, this approach has been prohibited in food-related applications due to the toxicity of those organic solvents. In other words, the synthetic polymer can improve the spinnability by modifying the physical properties of the mixture solution such as electrical conductivity, viscosity, or the degree of the chain entanglements or associations (Vega-Lugo et al, 2012). The

blend of whey protein with the synthetic polymer can be the approach to overcome the challenge of electrospinning of whey protein. To some extent, the electrospinning technique relies on the response of polymer solution in the electric field. Thus, the modification of solution properties (viscosity, conductivity, and surface tension) plays a critical role in the spinnability of polymers.

Dairy proteins such as whey and casein are considered as high-quality proteins with characteristics of convenience and are easily absorbable (McBean & Speckmann, 1998). It has been known that the electrospinning of dairy proteins (whey and casein) is a challenge due the complex secondary and tertiary structure, as well as weak internal interactions of dairy proteins (Ramazani et al, 2019). Generally, whey proteins are considered as unspinnable due to their complex secondary and tertiary structures, as well as the lack of entanglement induced by weak internal interactions (Ramazani et al, 2019). The whey protein-based nanofiber using electrospinning method has been developed for both independent spinning and spinning with a synthetic polymer (Vega-Lugo, & Lim, 2012).

Casein, as one of two major milk proteins, has been extensively studied for its application and physicochemical structure. Casein proteins are wildly used in beverages as nutritional supplements, thickeners, and texture stabilizers. Furthermore, casein proteins are considered as a drug and enzymatic delivery due to their structural features. Casein consists of four phosphoproteins family (αs1-, αs2-, β-, and κ-casein), and approximately 85% to 90% of casein in bovine milk exist as voluminous and spherical porous micelles (Chandan & Kilara, 2010). The proportions of αs1-, αs2-, β-, and κ-casein present as 4:1:4:1, and these fractions directly affect the ability to cross-link between casein and synthetic polymer in terms of structure, amino acid composition, and molecular weight differences (Ghosh, 2009). In the present study, the independent fabrication of casein nanofiber via electrospinning was considered nearly impossible

due to its complex secondary and tertiary structure, and the low resistances toward the entanglement of protein caused by weak chain interactions of polymer (Kriegel, guar Arrechi, Kit, McClements, & Weiss, 2008). Howbeit the spinnability of casein can be enhanced by the addition of a highly spinnable synthetic polymer or anionic surfactant (Selvaraj, Thangam, & Fathima, 2018). Over 55% of amino acids in casein contain polar side groups which provide extensive intra and inter-molecular hydrogen bonding, and those extensive intermolecular interactions induce insufficient viscoelasticity for electrospinning of casein (Selvaraj, Thangam, & Fathima, 2018). However, casein micelle possesses good stabilities against the denaturants (such as heat or urea) due to its lack of intrinsic structure (Fox and Kelly, 2018) and PVA powder dissolution requires long-term and high temperature (over 90℃ and 90 minutes dissolving time). Hence the combination of MCC and PVA could minimize the impact of temperature on the physicochemical structure of PVA and MCC during the dissolution.

The objective of this report is to overcome the difficulties of creating electrospun nanofiber based on dairy proteins, and to investigate the effects of dairy protein ingredient MCC and WPI with PVA mixture composition on the spinnability of MCC/PVA solution and the morphology of electrospun nanofiber.

Chapter2 Literature Review

Edible Film

In general, edible film are preformed thin layers formed on a food surface which consist of the edible material to protect food, and prevent migration of moisture, oxygen, and solute in or out of the food. Compared to synthetic packaging systems, edible film packaging systems are more advantageous because they are directly applied to the surface of the food as part of the food product; they can be eaten without having to open the package and without being disposed. It is also well established that edible film can be eaten as part of food, thus it is given the purpose of increasing nutritional value by modification of film composition. During the formation of edible film, the physical properties and functionalities of the film can also be modified by combining plasticizer and other additives with film forming biopolymers.

Technique of edible film preparation

The film-forming mechanisms of the edible film are intermolecular forces (covalent bond) or the electrostatic, hydrophobic, and ionic interactions (Han, 2014). Based on the preparation approach, the edible film can be classified as dry or wet-process. For the dry-process film such as thermoplastic extrusion (Kamal, 2019) include the process of heating, cooling, feeding, conveying, compressing, shearing, reacting, mixing, melting, homogenizing, amorphousizing, cooking, and shaping (Hernandez-Izquierdo & Krochta, 2008). In low moisture content conditions, the thermoplastic extrusion technique utilizes the thermoplastic properties of plasticized and heated polymers, while their glass-transition temperature is exceeded. On the other hand, wet-process is based on the film forming biopolymer dispersion. During the process, the polymers are dispersed into liquid phase within certain shape, and then dried in a low-moisture content environment. Compared to dry-process, the wet process involves dipping,

brushing, or spraying that allow liquid-form film material directly covering the surface of food, no matter surface is irregular or not. Besides, plasticizers play an indispensable role in proteins and polysaccharides-based edible film fabrication. It is low-molecular weight agents that aim to incorporate with biopolymers to increase their thermoplasticity and interrupt polymer by forming hydrogen bonds that can maintain distance between polymer within the polymer chains; or interacting with water to retain high moisture content and larger hydrodynamic radius of the edible film (Sothornvit & Krochta, 2001). Since the plasticizers can maintain distance and position themselves between polymers, they can improve the flexibility and processability of the film (Guilbert & Gontard, 1995).

Composition of edible film

Depending on the composition or the biopolymers, the edible film can be divided into following categories: proteins, polysaccharides, lipids, and composites edible film. Proteins as macromolecule materials with various functions given by specific amino acid sequences and molecular structures are wildly used in edible film formation. The characteristics of proteins include structure (secondary, tertiary, and quaternary), electrostatic charges, and amphiphilic nature that can be easily modified. To meet the functional requirements of edible film, the proteins are modified through treatments such as heat denaturation, pressure, irradiation, enzymatic treatment, or mechanical treatment (acids, alkalis, metal ions, salts, chemical hydrolysis, etc.) (Han, 2014). Protein-based edible films can be prepared by either animal or plant-based proteins including casein, whey proteins, gluten, soy protein or corn zein, etc. The protein derived essential micronutrients and amino acids also provide the benefit of increasing nutrient value of resulting edible film. Furthermore, the protein-based edible film has an

excellent sealing function of forming gas and moisture barriers, but poor water vapor resistance and tensile strength compared to lipids and polysaccharide-based film (Choi & Ha, 2001, Luo et al, 2022).

The polysaccharide, as simple monomer of film-forming materials include starch, non-starch carbohydrates, gums, and fibers which are mainly derived from agricultural feedstock or crustacean shell wastes (Kamal, 2019). Compared to proteins, the conformational structures of polysaccharides are more complicated and unpredictable due to their larger molecular weights. The numerous hydroxyl groups and hydrophilic moieties in the neutral carbohydrate structure leads to strong hydrogen bonds in film formation (Kumar, 2019). The plant polysaccharides such as pectin, carrageenan, agarose, alginates, and xanthan are capable of forming viscous or gelatinous colloids by absorbing a large amount of water, dissolving, and dispersing into the film (Kamal, 2019). Compared to the protein-based film, the polysaccharide-based edible film possesses excellent transparency and mechanical strength. Although, the polysaccharide-based edible film has a low sealing function but the highlight of its selective permeability to oxygen and carbon dioxide, and cost-effectiveness make it popular in the food industry.

Lipids, as well as resin, are edible biodegradable materials but not polymers that are highly deformable by modification of transition temperature between fluid, soft-solid, and crystalline-solid states. Compared to protein and polysaccharide-based film, edible films based on lipids are easier to be fabricated by casting and molding. The lipid-based edible film has high water resistance due to its hydrophobic nature, but it is also impressionable to temperature in terms of permeability (moisture and gas barrier efficiency) (Debeaufort & Voilley, 2009).

In various studies, researchers tend to mix various biopolymers together as emulsions or multi-layer coating. For example, the combination of lipid and protein (lipid layers on protein films) leads to higher temperature resistance and better mechanical strength (Debeaufort & Voilley, 2009). Thus, a variety of biopolymers can be mixed together to obtain the most desirable characteristic with unique functional properties. Another reason for the development of edible film is to fabricate edible film in combination with synthetic polymers.

Principle and Process of Electrospinning

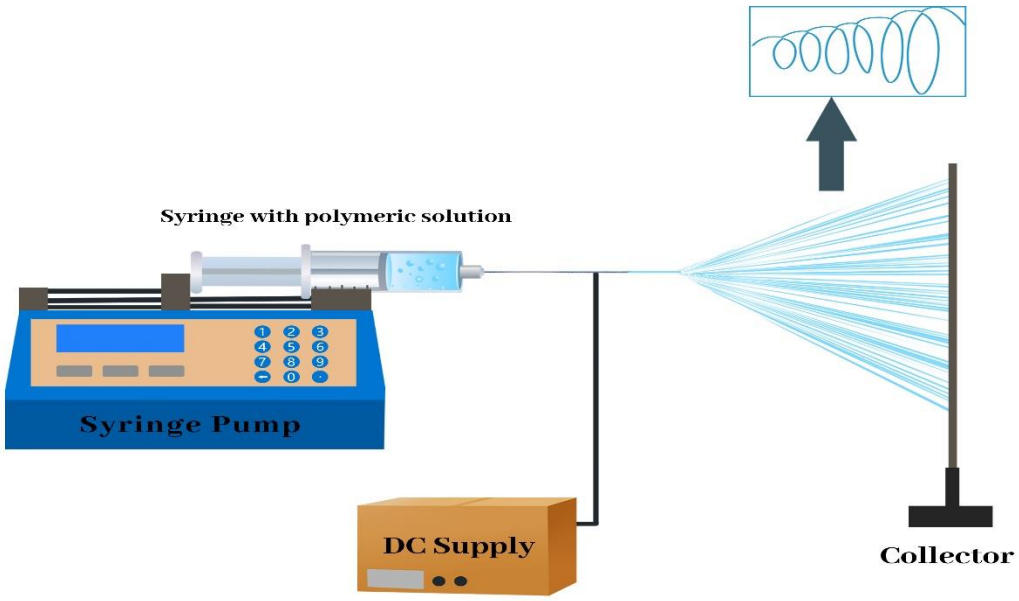

Fig. 2-1 Schematic illustration of the basic setup for electrospinning system. (Nieuwland et al, 2013).

Electrospinning is a technique of nanofiber fabrication by utilizing electrostatic repulsive force formed by a strong electric field to counteract the surface tension of the solution, suspension, or melt. The nanofiber formation by electrospinning can be divided into three successive steps: (i) To start the electrospinning process, a sufficient voltage is applied to the spinning solution in the syringe which creates an electric field between the tip of the syringe and

the counter electrode (the collector). The polymer droplet becomes electrostatically charged and has conical deformation on the tip of the syringe nozzle or needle which is called the Taylor cone. (ii) The onset of the Taylor cone leads to the polymer jetting; the development of bending instability, and a rectilinear jet elongation allows the jet to form a thin and long shape with spiraling and looping trajectories. (iii) As the electrostatic repulsive force between elements overcomes the surface tension, the polymer jet is leveled off (Xue, 2019). Solidification of the jet occurs within the period in a way that charged jet accelerates toward the counter electrode (collector) via evaporation of solvent or melt cooling which generates the nanofiber, and deposition of nanofibers as the final step in the electrospinning process is placed on the collector.

Experimental setups and needle type

Figure 2-1 provides a schematic diagram of a basic electrospinning instrument system which includes a high-voltage power supply, syringe pump, plastic syringes with different types of needles (metal-made spinneret), counter electrode or collector. A conductive collector can either act as a counter electrode or arranged as extra attachment next to the counter electrode. The electrical current of the power supply can be either direct current (DC) or alternating current (AC) within the range from a few hundred nano amperes up to several microamperes. Peristaltic or piston pump is used in the electrospinning system to control the flow rate of the polymer solution. The difference in flow rate is demonstrated by the physical characteristics of polymer solution including viscosity and conductivity. In general, the collector is placed 10-25 cm away from the primary electrode depending on the spinning situation (Agarwal, 2016). The collector is either stationary or rotating, the difference between these two collectors is the distribution of fibers. The fiber collected on the stationary collector is randomly oriented, while the fiber is aligned on the rotating collector.

Parameters controlling nanofiber formation

The successful nanofiber formation via electrospinning is determined by a series of parameters which can be divided into three sections: spinning solution characteristics, ambient conditions, and processing parameters (machine variables). The properties and characteristics of the polymer solution including viscosity, conductivity, molar mass, and surface tension significantly affect the condition of electrospinning and the morphology of the nanofiber. Generally, a polymer with high molecular weight (10^4-10^7g/mol), a viscosity (20-300,000cp), and a concentration of 10-20 wt.% can be used for electrospinning (Agarwal et al., 2016). The electrospinning process relies on the stretching of the charged polymer jet, and the concentration of polymeric solution significantly affects the stretching of a charged jet (Haider, A., Haider, S., & Kang, 2018). In presence of electric field and surface tension, the lack of sufficient polymer concentration leads to breaking entangled polymer chains into fragments, and these fragments induce the formation of the beaded fiber. Increasing the polymer concentration will result in an increase in viscosity, and also increase the chain entanglement among the polymer chain. A higher extent of polymer chain entanglements can overcome the surface tension and obtain uniform beadless nanofiber. However, increasing viscosity by increasing the polymer concentration to an exceeded value can also hamper the electrospinning process. The polymer solution can dry rapidly at the syringe tip and block it.

Electrical conductivity is a factor that describes the extent of how materials are willing to conduct charges, and it equals the reciprocal of specific electrical resistivity, and is proportional to current density and electric field strength. The conductivity of the solution can directly affect the formation of the Taylor cone and the diameter of the ultimate nanofiber. According to

various characteristics of polymer solution, it cannot confirm a proper conductivity for electrospinning system in terms of different concentrations, viscosity, pH, and temperature. In general, there is a range of conductivity (0.05-30 mS/m). To be specific, higher surface tension requires a higher conductivity, and an increase in conductivity contributes to the diameter reduction of fiber produced from the electrospinning process (Agarwal et al., 2016). Lower conductivity of solution can induce failure of Taylor cone formation due to no electrospinning. Similar to viscosity, increasing conductivity beyond a critical value(or applied exceeded voltage) can hinder the electrospinning process by forming multiple stretching jet from the surface of the charged droplet. In addition, irrespective to the interactions between polymers, most tof he inorganic ionic salts can be used for increasing the conductivity of the solution.

Furthermore, the flow rate of polymer solution fed to the nozzle is another important parameter. Any flow rate below or above the appropriate value can induce droplet, nozzle block (large droplet expose to air for a long time) splitter/thick or beaded fiber. The voltage applied to the spinning solution is mainly dependent on the electrode distance (distance between nozzle and collector) and electrode shape. In general, the distance is about 12 to 20, and the voltage applied is about 1kV per centimeter. It is always necessary to adjust the flow rate and other processing parameters (voltage, distance between nozzle and collector) to obtain a stable Tyler cone formation.

Overview of Dairy Ingredients

Casein, as one of the two major proteins in milk which exists as a form of porous and spherical micellar aggregates. Casein consists of four phosphoproteins family (αs1-, αs2-, β-, and κ-casein), and the fractions of each type of casein in micelle can directly affect the ability to cross-link between casein and synthetic polymer (Ghosh, 2009). The κ-casein is found on the

surface of the casein micelle which has the function of preventing infinite aggerates of the other three caseins by forming a protective coating around the spherical micelle. The diameter of casein micelles was found from 50 to 600nm with variations occurring based on fractions of various casein (De Kruif and Holt, 2003), and the amount of κ-casein. Due to the eliminated characteristic of κ-casein, the greater proportion of κ-casein in micelle, the smaller the casein micelle (Delacroix-Buchet et al. 1993).

Casein micelles are highly hydrated, during the production of concentrated milk products or skim milk powders, micelles are concentrated by either evaporation or membrane technology. While the size and composition of casein micelle can be accurately measured, there is still debate about the structure of the casein micelle. The submicelle and nanocluster models are the two major contenders' theories. Schmidt proposed the submicelle model in 1980, and hypothesized that casein micelle was formed by the aggregates of casein protein linked by calcium phosphate. The amount and function of the κ-casein directly support the submicelle theory. The quantitative difference of κ-casein divides aggregates(submicelle) into to two types (κ-casein rich and κ-casein poor), even though the existence of these two types of submicelles hasn't been proved (Schmidt, 1982). The self-aggregates characteristic of submicelle can gather into an individual casein micelle. As for the nanocluster model which proposed by Holt et al. (1992), the noncovalent interactions between casein phosphopeptide and calcium phosphate lead to the formation of small and clusters-form casein micelle. The growth of micelle is dependent on the cross-linkage of nanoclusters by phosphorylated αs1 and αs2 caseins. Due the lack of phosphate centers, it cannot participate in the formation of nanoclusters but only from a surface layer by associating with other interior aggregated casein (Dalgleish, 2011).

Stability and structure changes of casein micelle

The lack of intrinsic structures affords casein protein remarkable stability against the denaturant (heat and urea) (Fox and Kelly, 2004). However, the denaturation of the whey proteins and their interaction with casein micelles are the main factors that cause the instability of milk to heat. The heat below 100℃ does not cause the disruption of basic casein micelle structure, although κ-casein is dissociated from the heated micelle in an extensive manner as well as some αs-casein due to the increase of the electrostatic repulsion caused by increasing pH (Anema & Klosternmeyer, 1997). In other words, the heat stability of casein micelle in milk to large extent is dependent on the presence of whey protein. As the temperature is above 70℃, the denatured whey protein starts to aggregate, and forms complexes with κ-casein and αs2-casein which are distributed between the micelles and the serum. With increasing pH, less fraction of those complexes are attached to the surface of the micelle. Conversely, a higher number of complexes are bound to the micelles with a lower pH.

Micellar casein concentrate heat stability

The heat stability of micellar casein concentrates is highly affected by temperature and pH. As proposed by Sauer & Moraru in 2012, MCC is unstable in the sterilization range (temperature within 110 to 150°C, pH values of 6.5 to 7.3). MCC was visibly aggregated or coagulated at pH<6.7 after heating from 110 to 150°C, and there was barely casein micelle aggregated at pH>6.9 after heating. Thus, the extent of casein micelle dissociation increased with increasing pH after heating (Sauer & Moraru, 2012).

Whey protein isolate

Whey protein is the globular protein collected from the whey, as the by-product produced during cheese manufacture, and it has limited use in the dairy industry, such as protein powder or

protein bars. Whey protein is a complex mixture of globular protein molecules which consists of α-lactalbumin, β-lactoglobulin, serum albumin, immunoglobulins, and protease peptones. The conformational structure and functional properties of whey protein can be governed and modified by the changes in those globular folded structures. WPI (minimum protein content of 90%) is a common protein powder that is normally manufactured by ion-exchange chromatography or microfiltration of whey streams (Qi et al., 2011). The isolation of whey protein made by ultrafiltration is based on the size differences between molecules, while the WPI made by ion exchanges is dependent on the amphoteric characteristic of protein. Ultrafiltration is a cross-flow filtration process that utilizes pressure to concentrate whey protein by polymeric membranes, and the difference in WPI between the two techniques is the protein and mineral composition (absence of glycomacropeptides, lactoferrin and peptide fragments in ion-exchanged WPI).

Heat stability of whey protein

In the presence of calcium, the formation of intermolecular cross-link leads to the heat sensitivity of protein and its proximity to the molecules. However, regarding heat resistance of α-lactalbumin, the formation of intramolecular ionic bonds contributes to its heat resistance with the presence of calcium (Chandan & Kilara, 2010). Since β-lactoglobulin contains two disulfide bonds and one sulfhydryl group, its heat-induced sulfhydryl and disulfide interactions with α-lactalbumin enhance the heat sensitivity of α-lactalbumin. To a large extent, the thermal stability of whey protein is also affected by pH value. For example, α-lactalbumin possesses higher heat stability at pH ranges between 6.5 to 4.5 compared to pH of 3.5 for β-lactoglobulin (Bernal & Jelen, 1985). The significant point of whey protein interaction with polysaccharides is that the interaction between whey protein and polysaccharides can increase the resistance of β-

lactoglobulin to thermal denaturation, and protect the β-lactoglobulin from heat-induced solubility loss.

PVA (Polyvinyl alcohol)

PVA (polyvinyl alcohol), as a water-soluble synthetic polymer was used for surface modifications papermaking, and possesses commercial use of warp sizing in textiles, thickener, and emulsion stabilizers (Ramimoghadam et al., 2014). It is a carbon-carbon linked vinyl polymer that has the same linkage with plastics such as polyacrylamide, polypropylene, and polystyrene. PVA does not polymerize from vinyl alcohol as most vinyl polymers do, since vinyl alcohol tends to tautomerize to acetaldehyde due to its thermodynamic instability. Therefore, PVA is made by hydrolyzing polyvinyl acetate or sometimes other vinyl ester-derived polymers with chloroacetate or formate groups (Hallensleben, 2000).

In an electrospinning system, PVA has great spinnability which can produce a continuous fiber with diameters from nano amperes up to several microamperes using polymer solutions or melts. PVA also possesses excellent emulsifying and adhesive properties, and it is the reason PVA could associate with other polar polymers or nonpolar polymers (protein), thereby achieving the objective of conquering the electrospinning challenge of certain polymers. In addition, the degree of hydrolysis of PVA plays an important role in interacting with other polymers.

Chapter3 Methodology

Experimental design

The entire experiment was carried out in two phases. In the first phase, multiple methods were applied to the whey proteins and caseins to overcome the electrospinning difficulties. As designed, there were two methods of accomplishing the spinnability of dairy protein. Direct modification of dairy protein solution characteristics including viscosity, conductivity, and surface tension were considered as one of the methods. Sodium alginate (NaAlg), medium chain sodium hexametaphosphate (SHMP), and sodium chloride (NaCl) were added to the MCC solution, and denatured whey protein solution was acidified to pH 2. The blend of dairy protein with synthetic polymer (PVA) was another method to increase the spinnability of whey protein and casein. Since the feasibility of electrospun nanofiber fabrication based on the blend has been verified, the effects of PVA on the electrospinning of whey proteins were analyzed through the electrospinning of WPI/PVA blend with various concentrations.

In the second phase of the experiment, MCC with concentrations from 8% to 14% were blended with PVA at concentrations of 1%, 2%, and 3%. The MCC/PVA nanofibers were obtained through electrospinning. The characteristics including viscosity, conductivity and surface tension of the mixture were analyzed. The scanning electron microscopy further verified the structure of the MCC/PVA nanofibrous film and analyzed the effect of MCC/PVA ratios on the formation of nanofiber. All the experiments were done in triplicate.

Phase I

Materials

Chemicals including sodium alginate, medium chain sodium hexametaphosphate, platinum and sodium chloride were purchased from Thermo Fisher Scientific Inc. WPI were purchased from Leprino Foods Inc and MCC were purchased from Milk Specialties Global.

Solution preparation:

The WPI (whey protein isolate) and MCC (micellar casein concentrate) were selected as the dairy protein sources. For the MCC dispersions, sodium alginate (NaAlg), sodium hexametaphosphate (SHMP) and sodium chloride were respectively dissolved in MCC solution to increase the viscosity and conductivity, and their feasibility of electrospinning were verified. It has been reported that the addition of SHMP to micellar casein solution can increase its viscosity and turbidity (Pandalaneni et al, 2018).

WPI powder were dissolved in deionized water and stored overnight for complete rehydration. WPI solutions were heat denatured in the water bath for 2 hours. The concentration of whey protein was kept less than 6%.

WPI/PVA blend preparation

Material concentrations in all formulations were in a w/w basis. The WPI solutions were prepared at the concentration (2, 4, and 6% wt), and WPI was added slowly to the deionized water at 25℃ under stirring 200 rpm for one hour and stored in the refrigerator overnight to ensure complete rehydration. The WPI solutions were adjusted to pH 2 with HCl and denatured in 90 ℃ water bath for two hours, then cooled to the room temperature before used. The PVA powder (146000-186000 molecular weight) was added to the WPI solution at a concentration (4, 5, and 6% wt) and rehydrated for a minimum of 20 minutes under constant stirring at 200 rpm.

After the observation of PVA crystal expansion, the mixture of WPI and PVA was heated to 90℃ for one hour under stirring at 350 rpm. The solutions were then centrifuged (Thermo Fisher Scientific Marathon 21000R Multi-Purpose Benchtop Centrifuge, model # 64660557, Waltham, WA) at 5000 rpm for 15 minutes to remove the bubbles generated in the mixing procedure.

Surface tension measurement of WPI/PVA blend

The measurements were made using the DuNouy drop ring tensiometer (CSC Precision Tensiometer, model 70545; CSC Scientific Company, Inc., Fairfax, VA) at 30°C. The samples were placed in a 100 mL beaker and a clean ring was placed immersed into the solution. The reading starts to count at the point that the ring matches the upper surface of the solution until the interface between the solution and ring broken. The correction factor was calculated by the following formula:

$$F=0.0725+\sqrt{0.01452\times P/C^2 (D-d)} + 0.04534-1.679\, r/R^2$$

F= correction factor, P = apparent surface or interfacial tension (dynes per centimeter), C =ring circumference (centimeter), D =density of the lower phase (grams per cubic centimeter), d =density of the upper phase (grams per cubic centimeter), R =radius of the ring(centimeter), and r =radius of the ring wire(centimeter). Actual interfacial tension is calculated as P×F dynes/cm (Adapa, Schmidt, & Toledo, 1997).

Electrospinning of WPI/PVA blend

An electrospinning system consisting of a high-voltage power supply(PS35-PV) with a positive polarity between 0 and 40 kV, a syringe pump(NLS100), and a roll collector (ESD30s) were purchased from Nanolab Instruments Sdn. Bhd (21-G, 21, Jalan USJ 1/33, Taman Subang Permai, 47620 Subang Jaya, Selangor, Malaysia). The solutions were loaded in a 10ml syringe that was connected with a stainless-steel needle. A voltage of 14kV and a flow rate of 0.7 ml/h

were applied to the solution. Aluminum foil was used to collect the fibers which cover the roll collector, and the horizontal distance between needle tip and collector was 11 cm (Sullivan et al., 2014).

Phase II

MCC/PVA blend preparation:

Material concentrations in all formulations were in w/w basis. Blend of MCC and PVA were prepared at different concentrations (MCC: 8, 10, 12, 14% wt, PVA: 0, 1, 2, 3% wt.). The MCC powder was gradually added to the deionized water at 50℃ under stirring at 200 rpm for one and half hour solution. The PVA power (146000-186000 molecular weight) was added to the fully rehydrated MCC solution at a concentration (1, 2, 3%). After observing PVA crystal expansion, the blend of MCC and PVA was heated to 90℃ for 90 minutes under stirring at 350 rpm.

Electrospinning of MCC/PVA blend

Electrospinning systems are consisting of a high-voltage power supply with a positive polarity between 0 and 40 kV, a syringe pump, and a roll collector. The solutions were loaded in a 10ml syringe that was connected with a stainless-steel needle. A voltage of 14kV and a flow rate of 1.3 ml/h were applied to the solution. Aluminum foil was used to collect the fibers which cover the roll collector, and the horizontal distance between the needle tip and the collector was 11 cm (Tomasula et al., 2016).

Viscosity measurement:

Viscosity measurement of solutions was done using a rheometer (MCR-92 Anton Paar, Vernon Hills, IL) with ramping shear rate profile from 0.1 to 200 s^{-1} at 25 °C. The viscosity of solutions was reported at a shear rate of 100 s^{-1}.

Conductivity measurement

The conductivity measurements were made using a waterproof portable conductivity meter (Accumet AP75, Fisher Scientific, America)

Surface tension measurement

The surface tension of the solutions was measured by the surface tension meter (BZY-B (BZY102), Hubei Behemoth Technology Co., LTD) at room temperature with a 9.55mm radius platinum ring (Liu, Wang, & Li, 2020).

Fourier-transform infrared spectroscopy (FTIR) analysis

The functional group of nanofibers based edible films were investigated by a Nicolet summit FTIR (Thermo Fisher Scientific, Madison, WI, USA) with an average scan of 40 scans was taken for each sample to obtain infrared spectra at a resolution of 4 cm^{-1}.

Scanning electron microscope (SEM) analysis

The nanofiber collected on the aluminum foil was cut into rectangles of 5mm × 5 mm, and were sputter coated with approximately 2nm thick of platinum (Pt) using a Denton Vacuum Desk II cold sputter/etch unit (Moorestown, NJ 08057, USA). The morphology of the MCC/PVA-based nanofibers were analyzed by scanning electron microscopy (Hitachi S-3500N SEM) (Gandhi, Amamcharla, & Boyle, 2017). The mean diameter of nanofiber was measured with 30 randomly selected nanofibers from SEM images by using Image J e (Image J 1.42q, National Institutes of Health, US).

Statistical analysis

All the experiments were conducted in triplicates. The viscosity, conductivity, and surface tension results were expressed as means ± standard deviation (SD), and they were analyzed by

one-way analysis of variance (ANOVA) with Tukey tests to determine group differences, using SAS software (SAS Institute Inc).

Chapter4 Results & Discussion

Phase I

Feasibility of fabricating nanofiber from whey protein and micellar casein

Aqueous solutions of pure MCC were found to be impossible to electrospun into nanofiber under any ambient conditions or processing parameters. The addition of SHMP was expected to overcome this challenge. However, all the experiment trails failed to form fibers (Table 4-1). According to the observation of all experiments, the solution droplet at tip deformed to Taylor cone as polymer jet started to form, and pulled towards the counter electrode (collector). The electrospinning result of 10% MCC with 0.2% SHMP solution is shown in figures 4-1. Electrospinning of all the trails leads to the formation of beads and no fiber generated, and it caused by the globular structure of casein micelle, its high elasticity, strong intra-molecular hydrogen bonding which limits the free movement of casein (Tomasula et al., 2016). The liquid with high solvent content was observed on the foil paper, same results were obtained from all the experiment samples. Evaporation of solvent from jet surface generators fibers in electrospinning, and a large amount of solvent remaining on the foil directly indicated the failure of fiber formation (Wu et al, 2011).

During the 1st phase, multiple ingredients including SHMP NaAlg were directly added to the protein solution for modifying the physical characteristics of the solution (viscosity, conductivity, surface tension). All the test trails shown in the Table 4 1 were failed to generate nanofibers. The addition of SHMP and NaCl to the MCC solution was expected to overcome difficulties of electrospinning however, the physical characteristics of MCC solution was changed but it has no effect to its spinnability. Similarly, Extra NaAlg was added to WPI also proved to have no contributions to the spinnability of WPI solutions.

According to Table 4-2 and 4-3, a trace amount of SHMP to the pure MCC solution resulted in an increase in both viscosity and conductivity, and a considerable increase in viscosity of high MCC content solution was caused by the dissociation of casein micelle. The dissociation of casein micelle leads to diffusion of casein into the serum phase, and the calcium chelation and casein cross-links caused viscosity to increase (Pandalaneni et al, 2018).

Electrical conductivity determines the underlying force of a solution elongation towards the counter electrode which is an electrostatic repulsion force that is used to overcome the surface tension. An increase in the conductivity indicates that the surface charge increased, and repulsion forces were increased, and droplet subdivision occurs as a result of an increase in surface charge which overcomes the surface tension of the droplets. As shown in Table 4-3, all the samples had different degrees of viscosity increase, and these conductivity values were sufficient for the electrospinning process combing with the successful deformation of the Taylor cone and stable jet.

Table 4-1 Feasibility and Morphology of electrospinning product from modified protein solutions.

Protein solution	SHMP%	Feasibility of Electrospinning
6%MCC	0.1%	Unelectropinnable
	0.2%	Unelectropinnable
	0.2%	Unelectropinnable
8%MCC	0.1%	Unelectropinnable
	0.2%	Unelectropinnable
	0.3%	Unelectropinnable
10%MCC	0.1%,	Unelectropinnable
	0.2%	Unelectropinnable
	0.3%	Unelectropinnable
12%MCC	0.1%	Unelectropinnable
	0.2%	Unelectropinnable
	0.3%	Unelectropinnable
6%MCC	0.2% SHMP, 3% Nacl	Unelectropinnable
	0.3% SHMP,3% Nacl	Unelectropinnable
10%MCC	0.2% SHMP,3% Nacl	Unelectropinnable
	0.3% SHMP,3% Nacl	Unelectropinnable
	NaAlg%	
6%WPI	1%	Unelectropinnable
	2%	Unelectropinnable
8%WPI	1%	Unelectropinnable
	2%	Unelectropinnable

Table 4-2 Viscosity(mPa·s) of micellar casein concentrate dispersion with the addition of sodium hexametaphosphate (SHMP)

MCC	Sodium Hexametaphosphate Concentration (%)			
Concentration (%w/w)	0	0.1	0.2	0.3
6	1.53	2.16	4.17	4.70
8	2.83	3.46	4.36	7.25
10	4.02	20.17	45.35	100.88
12	7.19	34.78	124.27	214.41

Table 4-3 Solution properties and electrospinning feasibility of WPI/PVA solutions.

WPI%	PVA%	Viscosity (mPa·s)	Conductivity (ms/cm)	Surface tension mN/m	Feasibility
6%	0	1.212	1.37	33.71	Nonspinable
	1%	12.91	6.38	39.41	spinable
	2%	57.77	6.06	41.07	spinable
	3%	95.11	5.68	42.25	spinable
8%	0%	1.637	2.14	38.12	Nonspinable
	1%	247.18	7.25	44.22	spinable
	2%	401.91	6.9	46.41	spinable
	3%	1316.10	6.62	47.84	Nonspinable

Table 4-4 Conductivity(uS/cm) micellar casein concentrate dispersion with the addition of Sodium hexametaphosphate (SHMP)

MCC	Sodium Hexametaphosphate Concentration (%)		
Concentration (%w/w)	0.1	0.2	0.3
6	857	1078	1386
8	916	1128	1404
10	1008	1172	1470
12	919	1205	1530

Feasibility of fabricating nanofiber from WPI with PVA

As reported, interactions of synthetic polymers such as polyethylene oxide (PEO) with polymeric protein materials to produce electrospinnable blends has been studied (Lee et al, 2009). Even a high WPI concentration solution in acidic conditions could not form nanofiber, but the PVA was expected to act as a carrier which can result in the electrospinnability of WPI.

When PVA was added to WPI solution, a considerable increase in physical properties such as viscosity, conductivity, and surface tension was observed, especially the conductivity which means the interaction between whey proteins and PVA directly affects the conductivity and entanglement of the blend (Ramazani et al, 2019). However, continuously increasing PVA concentration led to a reduction of conductivity while viscosity and surface tension inversely increased. The 8%WPI with 3%PVA blend had an extremely high viscosity, and it induced a

rapid solidification at the tip of the syringe resulting in the failure of electrospinning. The surface tension of blends increased slightly with increasing PVA concentrations. Except for high viscosity-induced solidification, the repulsive electrostatic force created by the electric field on the droplet was sufficient to overcome the surface tension which owes to the high conductivity.

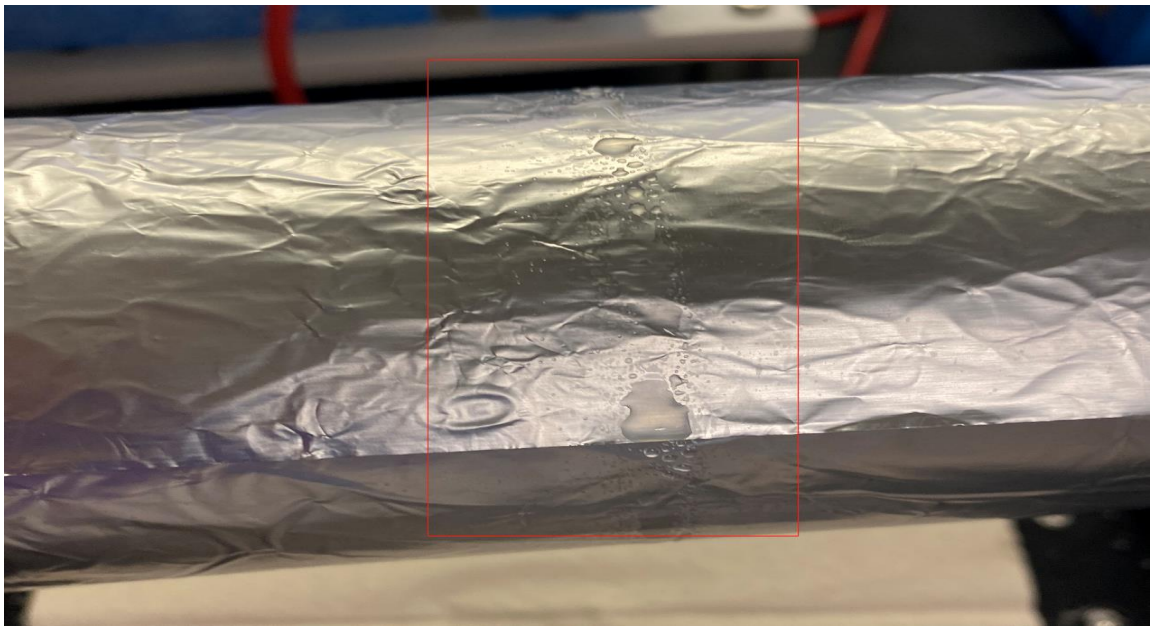

Fig. 4-1 Electrospinning result of 10%MCC with 0.2%SHMP.

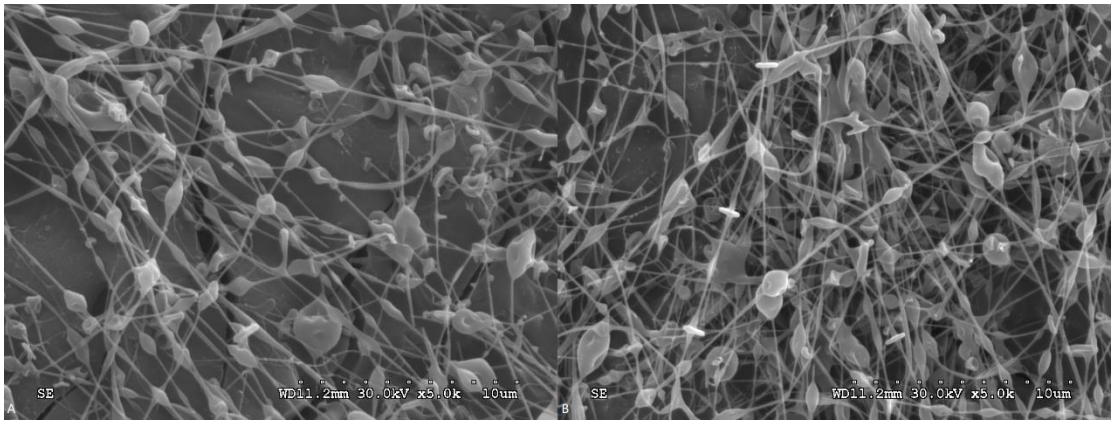

Fig. 4-2 Scanning electron micrographs of WPI-PVA electrospun fibers. A(left) 6%WPI/1%PVA, B(right), 8%WPI/1%PVA

Analysis of WPI/PVA solution

As shown in Figure 4-2, increasing WPI concentration from 6% to 8%, WPI solution with low PVA concentrations could form nanofiber. Numerous spherical beads were observed which might be considered as protein-rich fractions that lack interaction with synthetic polymers. In other words, the feasibility of fabricating nanofiber from WPI with PVA has been proved.

As previous hypothesis indicated, interactions of PVA with other protein materials could produce electrospinnable blend by carrying protein and incorporating it into subsequent fiber production which made the fabrication of whey protein-based electrospun nanofiber possible. Viscosity has been proved to play a critical role in the electrospinning process and nanofiber formation (Sukigara et al, 2003). According to Table.4-5, with a certain amount of PVA added to the WPI solution, the viscosity experienced a remarkable increase. The blend of WPI and PVA varied in concentrations range of spinnable viscosity ranging from 81.932 mPa.s to 558.025mPa.s. PVA act as a carrier, its inclusion in solution contributed to form an optimal viscosity which is a key factor for continuous nanofiber generation. In other words, the increase of viscosity and surface tension by the addition of PVA indicated the presence of interaction between WPI and PVA. In fixed concentration of WPI (6%), the effect of PVA leads to an excessive increase in the viscosity alone with the failure of electrospinning, A sticky appearances of solution and rapid solidification were observed at tip of the syringe. The viscosity and conductivity of WPI solution increased as function of its concentration whereas higher concentration of PVA with the same constant WPI concentration led to a decrease in electrical conductivity. Although higher conductivity of solution cause stronger electric field and lead to higher spinnability of solution, the final fiber formations of high PVA concentration but low conductivity were smooth and uniform which indicates final fiber formations were mainly affected by viscosity and surface tension. A low concentration and viscosity of polymer leads to

a spinnable solution governed by surface tension (Deitzel, Kleinmeyer, Harris, & Tan, 2001). In this study, surface tension of the solution increased with increasing both concentrations of WPI and PVA. In the lower viscosity solution such as 2% and 4% WPI with 4%PVA solution, the surface was overcome by the electrostatic force and formed a stable jet. It was mainly due to the sufficient spinnability support by high PVA concentration.

Thus, it could be concluded that increase in viscosity and surface tension coinciding with increase of either WPI or PVA concentration, while increasing PVA concentration led to the reduction of conductivity of the resulting solution. Addition of PVA improves the spinnability of WPI solution by modifying the physical properties of WPI solution.

Table 4-5 Physical characteristics of WPI-PVA solution

Solution (WPI: PVA) %wt	Viscosity mPa.s	Conductivity mS	Surface tension(mN/m)	Spinnability
2%WPI 4%PVA	81.932±15.078^{d}	2.953±0.201^{d}	22.328±1.526^{a}	Spinnable
2%WPI 5%PVA	189.617±39.833^{d}	2.847±0.086^{d}	27.325±1.232^{a}	Spinnable
2%WPI 6%PVA	362.463±50.238^{bcd}	2.573±0.032^{d}	31.958±2.828^{a}	Spinnable
4%WPI 4%PVA	124.854±33.61^{d}	4.087±0.401^{b}c	26.562±2.304^{a}	Spinnable
4%WPI 5%PVA	355.888±74.615^{cd}	3.797±0.214^{c}	30.186±1.273^{a}	Spinnable
4%WPI 6%PVA	558.025±67.461^{bc}	3.73±0.261^{c}	31.244±3.508^{a}	Spinnable
6%WPI 4%PVA	259.583±37.61^{cd}	5.53±0.017^{a}	33.519±5.867^{a}	Spinnable
6%WPI 5%PVA	759.063±15.323^{b}	5.31±0.182^{ab}	39.772±4.705^{a}	UnSpinnable
6%WPI 6%PVA	1057.767±11.998^{a}	4.987±0.035^{a}	44.293±2.513^{a}	UnSpinnable

Values with a different superscript letter in the same column indicate significantly different ($P < 0.05$).

Analysis of WPI/PVA electrospun nanofiber

Most of the combinations were spinnable and the nanofiber it produced were either beaded fiber (the nanofiber contains numerous beads and need to calculate the diameter of beads and fiber separately) or bead-less fiber (the nanofiber contains no beads or very few beads which can be ignored). Spinnability of blends were assessed based on the SEM images. According to figure 4-2, WPI solution with low PVA concentrations could form nanofiber alone with numerous

beads. However, a higher concentration of PVA did induce smooth fiber formation (figure 4-3), while a higher concentration of WPI led to the opposite effect. The nanofiber of a low concentration of WPI was well-distributed and has a diameter with a lower standard deviation. Since the concentration of WPI increased, there were more variances in the diameter of nanofiber, and it portrayed that WPI alone did not possess the effect of increasing spinnability. An increase of PVA concentration from 4 to 6% with 6%WPI wt led to the failure of electrospinning. To large extent, the excessive value of viscosity induced by whey protein acid gelation and PVA rehydration were one of the reasons that led to this situation. On the other hand, fast solidification of the mixture solution at the tip of the syringe blocked the jet and obstructed the flow of the blend solution. The flow rate was not sufficient to push out all the solutions inside the needle within the time of solution solidification. In addition, the liquid drop formed on the syringe tip was exposed to air which also accelerated the gelation and solidification of the blend solution.

Another factor that contributed to differences in nanofiber morphologies in Fig.4-3 was the protein configuration (Vega‐Lugo & Lim, 2012). WPI adopted a globular conformation in a neutral solution which limited its interactions with PVA. By contrast, in acidic environments, whey proteins were likely to unfold, allowing WPI-PVA chain entanglements.

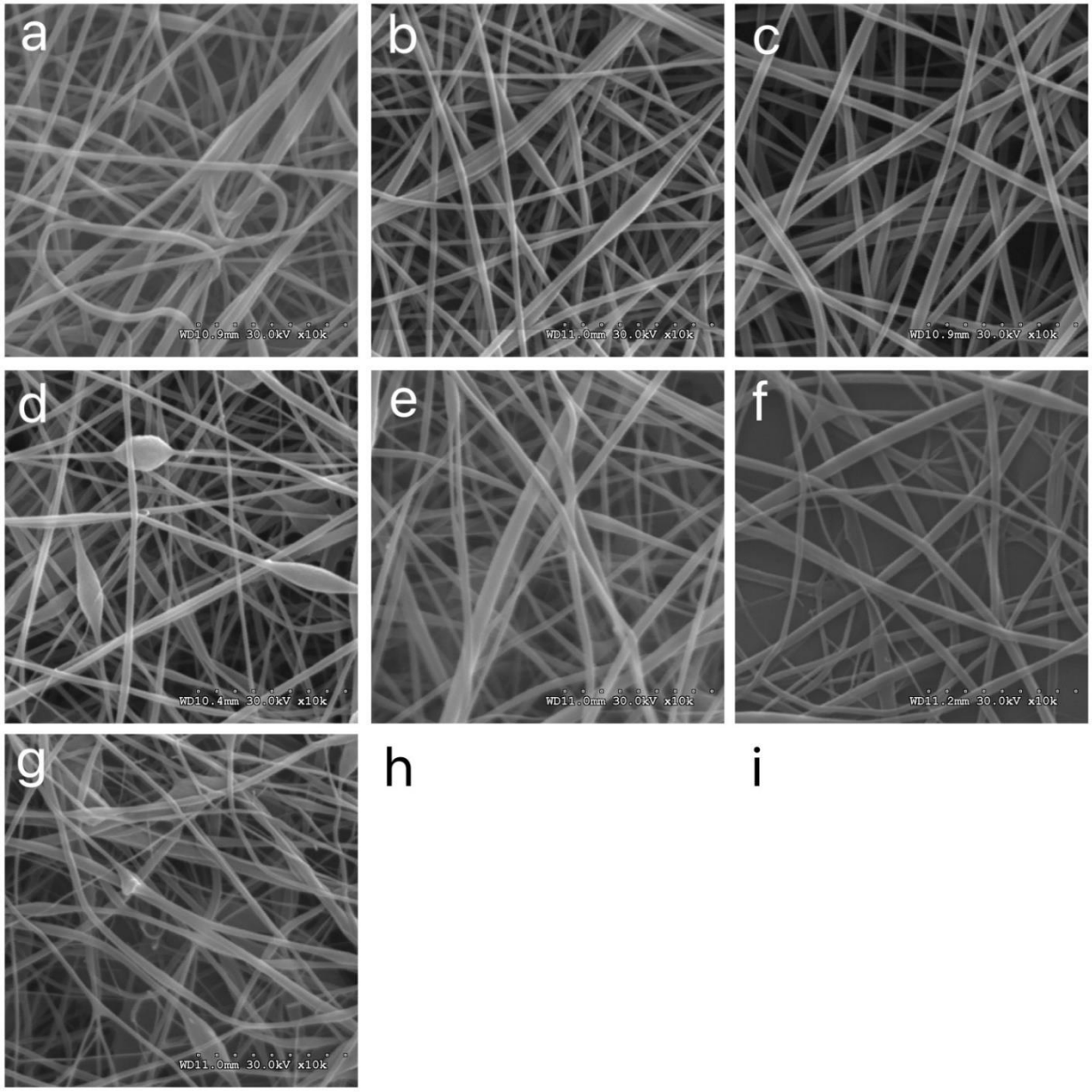

Fig. 4-3 The SEM image of electrospun fiber of mixture of WPI-PVA solutions under pH=2. The row represented of PVA concentration (4,5,6% wt) and the column represented the WPI concentration at resolution 5μm. The image h and I represent that the 6% WPI with 5% and 6% PVA were failed to form nanofiber which is blank.

Phase II

Analysis of physicochemical properties of MCC/PVA blend

Pure casein micelle solution cannot by directly fabricate nanofiber through electrospinning, even blend with specific ingredients (SHMP, NaAlg, NaCl) that can modify the physical characteristics of casein micelle solution. It requires a carrier polymer such as PVA that enable to decrease the tendency of intermolecular chain bonding in casein micelle.

To examine the effect of blend composition on the spinnability of MCC/PVA solution and the morphology of nanofiber, various concentrations of MCC (8,10,12, and 14% wt) and PVA (0,1,2, and 3% wt) were used in this experiment. The viscosity, conductivity, and surface tension for the interpretation of spinnability of MCC-PVA solution are shown in Table 4-6.

The successful nanofiber formation via electrospinning is determined by a wide range of parameters which can be divided into three sections: material parameters, ambient conditions, and processing parameters (machine variables). Viscosity and conductivity are two main material parameters that affect the electrospinning process and nanofiber formation. As expected, the apparent viscosity of the MCC and PVA blend increased significantly with an increase in MCC and PVA concentration at a shear rate of 100^{-1}. Compared to the pure MCC solution, there is a remarkable increase in the viscosity whereas the addition of PVA to the MCC solution. The pure 14% MCC solution showed a viscosity of and it increased to 32.23 mPa/s with 1% addition PVA, and it apparently increased to 359.09 mPa/s for the 8%MCC:3%PVA. Although the combination of lower molecular weight casein micelle and high molecular weight PVA should lead to a decrease in viscosity (Oroumei, Fox & Naebe, 2015), the viscosity of MCC-PVA solution still increased while the MCC concentration increased. Furthermore, A significant increase in viscosity and surface tension was observed in WPI solutions when PEO was added

which indicates the presence of interactions between the two polymers. In addition, there was the observation of tip block due to the rapid solidification of MCC-PVA solution which could impede the process of constant electrospinning. The excessively increased viscosity causes a challenge during the stretching process on the tip. The significant increase in viscosity can retard the stretching ability of the electrical field, and lead to the ultimate increase in fiber diameter (Deng, Kang, Liu, Feng, & Zhang, 2017).

Similarly, an increase in conductivity is also attributed to the higher content of MCC and PVA in the MCC: PVA blend. The value of conductivity increased with increased MCC and PVA concentration, as did the viscosity value. In regard to 1% PVA concentration and the MCC content from 8 to 14%, the conductivity significantly increased from 424.67 to 550 mS/Cm, while the addition of PVA only had a slight impact on the conduction. Within a 14% MCC solution, the addition of PVA from 1% to 3% led to a slight rise from 550 to 570 mS/Cm. Addition of PVA to the fixed high concentration of casein micelle did not significantly increase the conductivity, especially in 12% and 14% casein micelle solution. For example, there are also no significant differences between the conductivity of 14%MCC with 2%PVA and 3% PVA, and the 12%MCC with 2%PVA and 3%PVA, respectively. Hence the concentration of MCC plays a more dominant role in controlling the conductivity of the blend. As the conductivity increases, more free ions lead to more charges carried mutually repulsive in the jet, and it makes the jet subject significantly stronger stretching in the electric field (Kriegel, C., Arrechi, A, 2008).

Generally, electrospinning requires a low surface tension to initiate the formation of a polymer jet, which reduces the electric field strength required. As a fact, the addition of MCC and PVA has a slightly enhancing effect on surface tension which can be counteracted by the

remarkable increase of viscosity and conductivity. The statistical results suggest the lack of significant differences between the mean of surface tension.

Table 4-6 Physical characteristics of MCC-PVA solution

Solution (MCC:PVA %wt)		Viscosity (mPa/s)	Conductivity (uS/Cm)	Surface Tension (mN/m)
8	0	3.523 ±0.416	378.833 ±1.169	48.032 ±0.142
	1	8.430 ±0.444^{h}	424.667 ±8.505^{g}	49.074 ±0.281^{e}
	2	26.413 ±1.664^{fgh}	468.000±10.000^{f}	49.220 ±0.359^{e}
	3	76.486 ±7.684^{de}	495.667 ±6.506^{de}	49.588 ±0.283^{de}
10	0	4.171 ±0.382	433.25 ± 5.285	48.199 ±0.072
	1	11.699 ±0.595^{gh}	476.333 ±8.327^{ef}	49.333±0.3045^{e}
	2	40.460 ±0.454^{f}	515.667 ±3.512^{d}	49.206±0.657^{e}
	3	124.423 ±2.829^{c}	532.000 ±1.732^{bc}	50.302±0.275^{bd}
12	0	7.127 ±0.245	471.333 ±4.546	48.355 ±0.252
	1	20.471 ±1.348^{fgh}	522.667±17.926^{c}	49.683±0.464$_{de}$
	2	72.700 ±5.848^{e}	559.333±12.858^{ac}	50.400±0.567^{b}
	3	191.457 ±5.371^{b}	556.667 ±7.572a	50.882±0.265^{b}
14	0	13.02 ±0.632	497.167 ±3.489	48.784 ±0.088
	1	32.229±3.332^{fg}	550.000±5.000^{ab}	49.082±0.153^{e}
	2	93.892±4.870^{d}	569.000±15.716^{a}	49.708±0.193^{de}
	3	359.088±33.459^{a}	570.000±5.292^{a}	51.721±0.436^{a}

Values with a different superscript letter in the same column indicate significantly different ($P < 0.05$).

Morphological analysis of MCC/PVA nanofibers

Morphology of electrospun MCC-PVA nanofibers were assessed based on the SEM images as shown in Fig. 4-4. The ultrafine nanofibers observed in Fig. 4-4 (a,d,g,j,b,e, and h) represent the PVA-rich domain while the spherical beads to some extent are protein-rich fractions. Regarding those bead-free nanofibers in Fig. 4-4 (h,k,c,f,i, and l), casein micelles could be considered as the spherical ball which has the exclusion of each other due to the negative charges on the surface of κ-casein, and PVA acted as padding filling the gap between each casein micelles.

According to Figure 4-4, the phase transitions of nanofibers from nonhomogeneous beaded nanofibers to bead-free uniform nanofibers were due to the increasing concentration of both MCC and PVA. In other words, a higher concentration of both MCC and PVA helps to eliminate beads. The beads formations are related to the lack of chain entanglements. As displayed in Fig 4-4.a-c, there is a remarkable decrease of beads formation alone with higher PVA concentration However, Fig 4-4. a, d, g, and j showed no apparent changes in bead formation, while smooth nanofiber with bead reduction were observed from Fig 4-4. b, e, h, and k. Accordingly, the function of eliminating bead formation of MCC requires a minimum concentration of PVA or it could conclude that MCC alone did not possess the effect of increasing spinnability. Fine, smooth, uniformly sized nanofiber were generated from the blend with over 2% PVA.In addition, the viscosity and conductivity of 10%MCC with 2%PVA are lower than 8%%MCC with 2%PVA, while the surface tension is opposite. Therefore, it can be concluded that an increase in solution viscosity and conductivity coinciding with a decrease in solution surface tension supports the formation of smooth beads-free nanofiber.

The interaction between protein and synthetic polymer changes the functional properties and physicochemical structure of the blend. The entanglement of casein micelle is critical to the formation of nanofibers. If casein micelles were not entangled, beads or droplets instead of nanofibers are typically deposited on the collector plate which is the same as nanofiber in Fig. 4-4 (a,d,g,j,b,e, and h). According to previous research, PVA is capable of nanofiber formation, and it can enhance the entanglement of casein micelle (Biranje, Madiwale, & Adivarekar, 2019). In 8%MCC with 1%,2% 3% PVA, and 10%MCC with 1%PVA solution, the chain entanglements may not be enough which caused the bead nanofiber formation with larger

diameters. Since the casein micelle was replaced by PVA (higher PVA concentration), the morphologies of nanofibers changed from beaded nanofiber to a smooth fibrous structure which indicates PVA itself is capable of enhancing molecular entanglements.

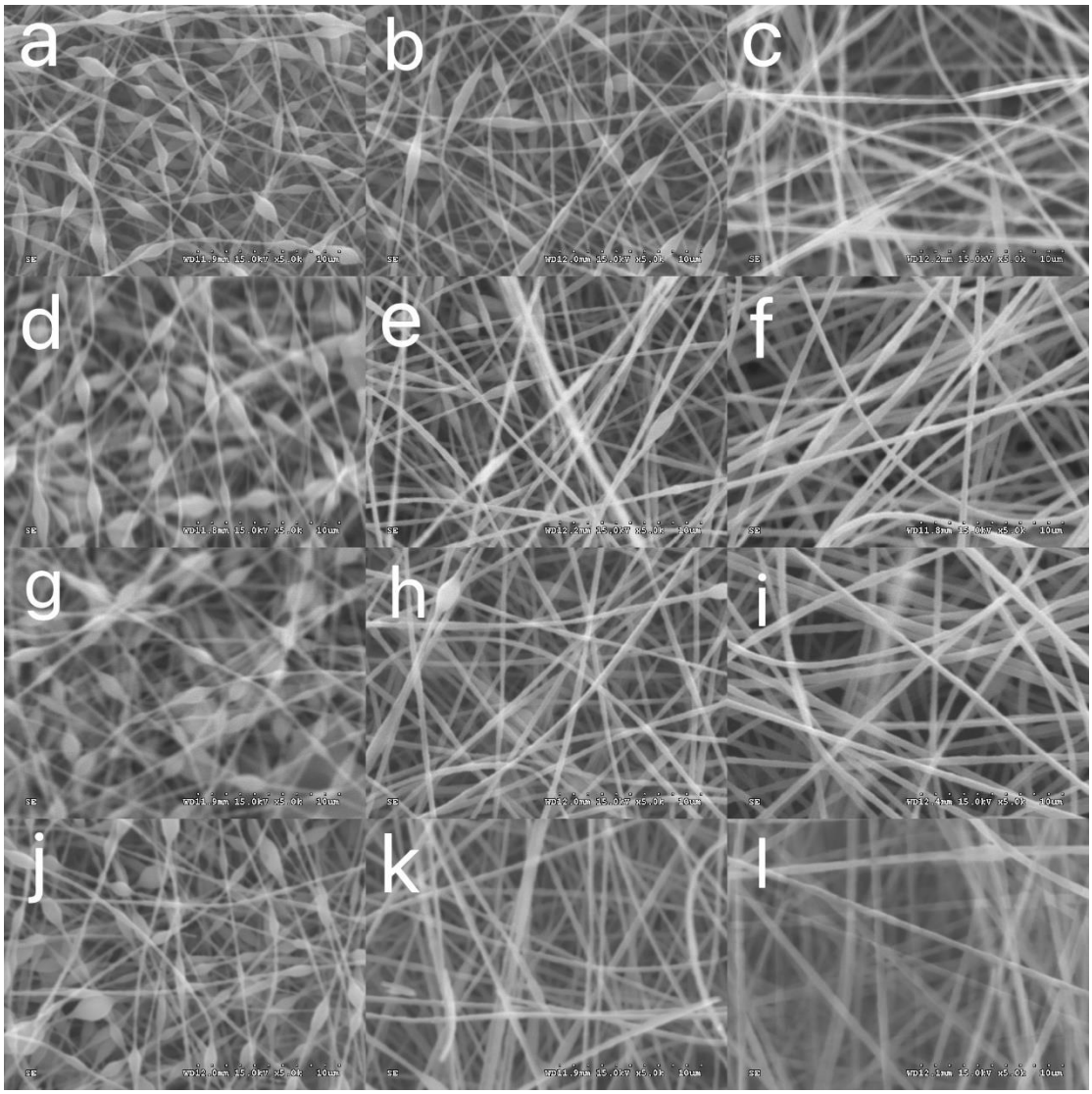

Fig. 4-4 Scanning electron microscope of MCC-PVA nanofiber. The SEM image of electrospun nanofiber of the blend of MCC-PVA solutions at different concentrations. The column represent the PVA concentration (1,2,3,% wt) and the row represent the MCC concentration

With regard to the diameter of the beaded nanofiber, as expected, the nanofiber diameter increase as the total polymer concentration increases, but higher concentrations of PVA and MCC lead to the reduction of beaded nanofiber diameter while higher concentrations of MCC and PVA have the opposite effect in bead-free nanofiber. For example, the diameter of 8%MCC/1%PVA beaded nanofiber (984.467nm) were larger than 8%MCC/2%PVA beaded nanofiber (822.533nm) and 10%MCC/1%PVA beaded nanofiber (858.4nm). The results from Table 4-7 indicate that the bead diameter of 8%MCC-1%PVA (984.467±137.607nm) was decreased with 2% PVA (822.533±114.26), while the nanofiber diameter of the same concentration was increased (From 182.333±29.81 to 216.600±30.5). The average nanofiber diameters of fixed PVA concentrations were only slightly increased with higher MCC concentrations, whereas there were significant differences in diameter among all three PVA concentrations within the same MCC concentration. The increase in the nanofiber diameter could be mainly due to the increase in the solution viscosity which was caused by the higher content of PVA, while the nanofiber diameter slightly increased when MCC concentration increased.

Table 4-7 the diameter of nanofiber at different concentrations of MCC/PVA

Solution (MCC:PVA %wt)		Fiber Status	Diameter (nm)	Fiber Status	Diameter (nm)
8	1	Nanofiber	182.33±29.806^{bcd}	Beads	984.47±137.61^{a}
8	2	Nanofiber	216.60±30.500^{bc}	Beads	822.53±114.26^{b}
8	3	Nanofiber	352.93±26.095^{f}		
10	1	NanofiberA	261.40±26.101^{ab}	Beads	858.40±125.52^{bc}
10	2	Nanofiber	338.00±49.038^{cdef}		
10	3	Nanofiber	461.60±19.018^{ef}		
12	1	Nanofiber	259.67±31.151^{a}	Beads	868.00±92.01^{c}
12	2	Nanofiber	371.87±41.217^{f}		
12	3	Nanofiber	502.80±53.224^{def}		
14	1	Nanofiber	217.33±33.109^{ab}	Beads	823.40±159.23^{b}
14	2	Nanofiber	390.00±33.287^{ef}		
14	3	Nanofiber	582.80±61.163^{cde}		

Values with a different superscript letter in the same column indicate significantly different (P＜0.05).

FTIR analysis

The objective of FTIR measurement was to verify the presence of casein micelle in electrospun nanofiber film. According to the previous literature and Fig. 4-5, the characteristic absorption band of ‒CONH– (amide I) at 1640 cm^{-1}, ‒NH– (amide II) at 1540 cm^{-1}, along with –CH– band 3340 cm^{-1} indicate the presence of micelle casein in micellar casein/PVA electrospun nanofiber (Biranje, Madiwale, & Adivarekar, 2019). With the increase of MCC concentrations, the absorption band at 1640 and 1540 cm^{-1} were also enhanced. From Fig 4-5, a large band between 3550 and 3300 was observed which is the O–H stretching overlapping with N–H stretching.

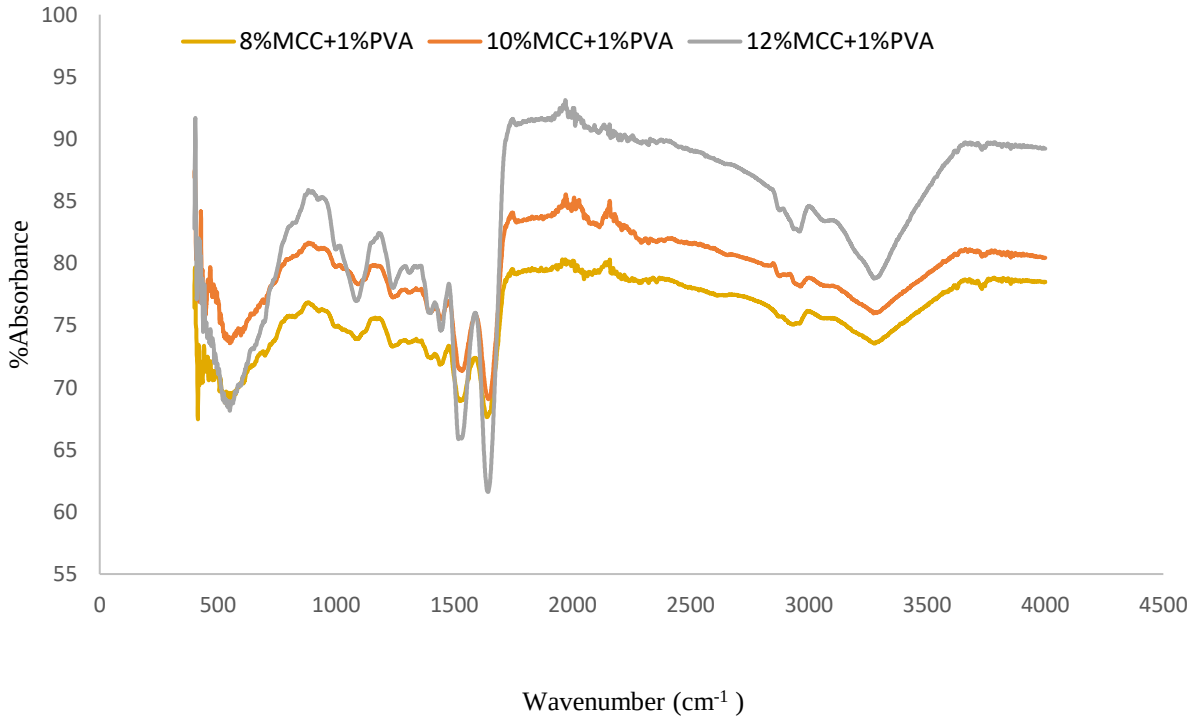

Fig. 4-5 FTIR spectrum of electrospun nanofiber film of MCC/PVA with ratio 1%PVA+ 8%, 10%,12%MCC.

Chapter5 Conclusion

The single modification of solution parameters is not feasible, even though the viscosity and conductivity had been promoted. In addition, the higher conductivity of the MCC solution caused better electrospinnability, but the final fiber formation of the solution was still affected by viscosity and surface tension. The feasibility of fabricating nanofiber from WPI with PVA has been proved, and the feasibility of overcoming the electrospinning challenges of dairy protein by blending with synthetic polymer has also been proven.

The addition of PVA to the WPI solution increased the viscosity and surface tension indicating the interactions between WPI and PVA. However, the addition of PVA had the opposite effect on electrical conductivity. A higher concentration of PVA eliminated bead formation while a higher concentration of WPI did not have this effect. In other words, bead-free fiber could be generated or correlated with relatively higher viscosity and lower conductivity. Alteration in secondary structures by adjusting pH to 2 had an effect on the solution properties and morphology of electrospun nanofibers.

The solution rheology and spinnability were conducted by measuring the physical characteristics (viscosity, conductivity, and surface tension) of the blend. The successful fabrication of food-grade nanofiber based on casein micelle and polyvinyl alcohol. Increasing the concentration of both MCC and PVA contributes to the spinnability of the blend solution. According to the statistical analysis in Table 4-6, the modification of the blend ratio does not make a significant difference in surface tension. Increasing the concentration of both MCC and PVA eliminates the beads formation, and as a result, fine beads-free nanofibers with uniform size were generated with a minimum concentration of 2% PVA. A higher concentration of PVA alone with a low concentration of MCC led to the reduction of beaded fiber diameter while a

higher concentration of MCC had the opposite effect. The excessively high viscosity could hinder the electrospinning process which was embodied in increasing nanofiber diameter.

Electrospinning of dairy protein is considered as the method of fabricating food-grade edible film. As mentioned in previous discussion, we developed the food-grade nanofiber used for the edible film. The feasibility of blending dairy protein with synthetic polymer PVA could overcome the challenge of electrospinning of dairy protein. Combined with the SEM images and analysis of the physical characteristics of blend solutions, the optimal ratio of MCC and PVA was established (12%MCC/3%PVA). The concentration of PVA plays a dominant role in the generation of smooth nanofiber. By contrast, the effect of MCC concentration on eliminating bead formation requires a minimum concentration, and higher WPI possesses an opposite effect on smooth nanofiber formation.

However, the dairy protein-based nanofiber cannot be directly used as edible film material so far due to its high adhesion and soft texture. In addition, these nanofibers could wrap food material which is type of wet process approach of edible film making. This function needs further testing for its permeability, solubility and adhesion. Since higher concentration of PVA contribute to the morphology of nanofiber, further investigations may focus on higher PVA concentration ratio for solving the texture problem of nanofiber film.

References

Wen, P., Zong, M. H., Linhardt, R. J., Feng, K., & Wu, H. (2017). Electrospinning: A novel nano-encapsulation approach for bioactive compounds. Trends in Food Science & Technology, 70, 56-68.

McBean, L. D., & Speckmann, E. W. (1988). Nutritive value of dairy foods. In Fundamentals of dairy chemistry (pp. 343-407). Springer, Boston, MA.

Ramazani, S., Rostami, M., Raeisi, M., Tabibiazar, M., & Ghorbani, M. (2019). Fabrication of food-grade nanofibers of whey protein Isolate–Guar gum using the electrospinning method. Food Hydrocolloids, 90, 99-104.

Han, J. H. (2014). Edible films and coatings: a review. Innovations in food packaging, 213-255.

Kamal, I. Edible Films and Coatings: Classification, Preparation, Functionality and Applications-A Review. Arc Org Inorg Chem Sci 4 (2)-2019. AOICS. MS. ID, 184.

Sothornvit, R., & Krochta, D. J. (2000). Plasticizer effect on oxygen permeability of β-lactoglobulin films. Journal of Agricultural and Food Chemistry, 48(12), 6298-6302.

Guilbert, S., Gontard, N., 1995. Edible and biodegradable food packaging. In: Ackermann, P., Ja¨gerstad, M., Ohlsson, T. (Eds.), Foods and Packaging Materials—Chemical Interactions. The Royal Society of Chemistry, Cambridge, U.K, pp. 159-168.

Hernandez-Izquierdo, V. M., & Krochta, J. M. (2008). Thermoplastic processing of proteins for film formation—a review. Journal of food science, 73(2), R30-R39.

Choi, W. S., & Han, J. H. (2001). Physical and mechanical properties of pea-protein-based edible films. Journal of Food Science, 66(2), 319-322.

Luo, S., Chen, J., He, J., Li, H., Jia, Q., Hossen, M. A., ... & Liu, Y. (2022). Preparation of corn starch/rock bean protein edible film loaded with d-limonene particles and their application in glutinous rice cake preservation. International Journal of Biological Macromolecules, 206, 313-324.

Kumar, N. (2019). Polysaccharide-based component and their relevance in edible film/coating: A review. Nutrition & Food Science.

Debeaufort, F., & Voilley, A. (2009). Lipid-based edible films and coatings. In Edible films and coatings for food applications (pp. 135-168). Springer, New York, NY.

Xue, J., Wu, T., Dai, Y., & Xia, Y. (2019). Electrospinning and electrospun nanofibers: Methods, materials, and applications. Chemical reviews, 119(8), 5298-5415.

Agarwal, S., Burgard, M., Greiner, A., & Wendorff, J. (2016). Electrospinning. De Gruyter.
De Kruif, C. G., & Holt, C. (2003). Casein micelle structure, functions and interactions. In Advanced dairy chemistry—1 proteins (pp. 233-276). Springer, Boston, MA
.
Ghosh, A., Ali, M. A., & Dias, G. J. (2009). Effect of cross-linking on microstructure and physical performance of casein protein. Biomacromolecules, 10(7), 1681-1688.

Delacroix-Buchet A, Lefier D, Nuits-Petit V. 1993. Polymorphisme de la caseine ´ κ de trois races bovines francaises et aptitude a la coagulation. Lait 7:61–72

Schmidt DG. 1982. Association of caseins and casein micelle structure. In Developments in Dairy Chemistry, ed. PF Fox, 1:61–86. London: Appl. Sci. Publ.

Dalgleish DG. 2011. On the structural models of casein micelles: review and possible improvements. Soft Matter 7:2265–72

Huppertz, T., Fox, P. F., & Kelly, A. L. (2004). High pressure treatment of bovine milk: effects on casein micelles and whey proteins. Journal of dairy research, 71(1), 97-106.

Anema SG, Klostermeyer H. 1997. Heat-induced, pH dependent dissociation of casein micelles on heating reconstituted skim milk at temperatures below 100◦C. J. Agric. Food Chem. 45:1108–15

Sauer, A., & Moraru, C. I. (2012). Heat stability of micellar casein concentrates as affected by temperature and pH. Journal of dairy science, 95(11), 6339-6350.

Qi, P. X., & Onwulata, C. I. (2011). Physical properties, molecular structures, and protein quality of texturized whey protein isolate: Effect of extrusion moisture content. Journal of Dairy Science, 94(5), 2231-2244.

Chandan, R. C., & Kilara, A. (Eds.). (2010). Dairy ingredients for food processing. John Wiley & Sons.

Bernal, V., & Jelen, P. (1985). Thermal stability of whey proteins–a calorimetric study. Journal of Dairy Science, 68(11), 2847-2852.

Ramimoghadam, D., Bagheri, S., & Abd Hamid, S. B. (2014). Progress in electrochemical synthesis of magnetic iron oxide nanoparticles. Journal of Magnetism and Magnetic Materials, 368, 207-229.

Hallensleben, M. L. (2000). Polyvinyl compounds, others. Ullmann's Encyclopedia of Industrial Chemistry.

Park, J. C., Ito, T., Kim, K. O., Kim, K. W., Kim, B. S., Khil, M. S., ... & Kim, I. S. (2010). Electrospun poly (vinyl alcohol) nanofibers: effects of degree of hydrolysis and enhanced water stability. Polymer journal, 42(3), 273-276.

Zhang, C., Li, Y., Wang, P., & Zhang, H. (2020). Electrospinning of nanofibers: Potentials and perspectives for active food packaging. Comprehensive Reviews in Food Science and Food Safety, 19(2), 479-502.

Shenoy, S. L., W. D. Bates, H. L. Frisch, and G. E. Wnek. 2005. Role of chain entanglements on fiber formation during electrospinning of polymer solutions: good solvent, non-specific polymer-polymer interaction limit. Polymer (Guildf.) 46:3372–3384.

Vardhanabhuti, B., & Foegeding, E. A. (1999). Rheological properties and characterization of polymerized whey protein isolates. Journal of Agricultural and Food Chemistry, 47(9), 3649-3655.

Wu, X. F., Salkovskiy, Y., & Dzenis, Y. A. (2011). Modeling of solvent evaporation from polymer jets in electrospinning. Applied Physics Letters, 98(22), 223108.

Roefs, S. P., & De Kruif, K. G. (1994). A model for the denaturation and aggregation of β-lactoglobulin. European Journal of Biochemistry, 226(3), 883-889.

Pandalaneni, K., Amamcharla, J. K., Marella, C., & Metzger, L. E. (2018). Influence of milk protein concentrates with modified calcium content on enteral dairy beverage formulations: Physicochemical properties. Journal of dairy science, 101(11), 9714-9724.

Lee, K. Y., Jeong, L., Kang, Y. O., Lee, S. J., & Park, W. H. (2009). Electrospinning of polysaccharides for regenerative medicine. Advanced drug delivery reviews, 61(12), 1020-1032.

Ramazani, S., Rostami, M., Raeisi, M., Tabibiazar, M., & Ghorbani, M. (2019). Fabrication of food-grade nanofibers of whey protein Isolate–Guar gum using the electrospinning method. Food Hydrocolloids, 90, 99-104.

Chandan, R. C., & Kilara, A. (Eds.). (2010). Dairy ingredients for food processing. John Wiley & Sons.

Ghosh, A., Ali, M. A., & Dias, G. J. (2009). Effect of cross-linking on microstructure and physical performance of casein protein. Biomacromolecules, 10(7), 1681-1688.

Ramazani, S., Rostami, M., Raeisi, M., Tabibiazar, M., & Ghorbani, M. (2019). Fabrication of food-grade nanofibers of whey protein Isolate–Guar gum using the electrospinning method. Food Hydrocolloids, 90, 99-104.

Vega-Lugo, A. C., & Lim, L. T. (2012). Effects of poly (ethylene oxide) and pH on the electrospinning of whey protein isolate. Journal of Polymer Science Part B: Polymer Physics, 50(16), 1188-1197.

Shenoy, S. L., Bates, W. D., Frisch, H. L., & Wnek, G. E. (2005). Role of chain entanglements on fiber formation during electrospinning of polymer solutions: good solvent, non-specific polymer–polymer interaction limit. Polymer, 46(10), 3372-3384.

Agarwal, S., Burgard, M., Greiner, A., & Wendorff, J. (2016). Electrospinning. De Gruyter.

Xue, J., Wu, T., Dai, Y., & Xia, Y. (2019). Electrospinning and electrospun nanofibers: Methods, materials, and applications. Chemical reviews, 119(8), 5298-5415.

Vasita, R., & Katti, D. S. (2006). Nanofibers and their applications in tissue engineering. International Journal of nanomedicine, 1(1), 15.

Selvaraj, S., Thangam, R., & Fathima, N. N. (2018). Electrospinning of casein nanofibers with silver nanoparticles for potential biomedical applications. International journal of biological macromolecules, 120, 1674-1681.

Kriegel, C., Arrechi, A., Kit, K., McClements, D. J., & Weiss, J. (2008). Fabrication, functionalization, and application of electrospun biopolymer nanofibers. Critical reviews in food science and nutrition, 48(8), 775-797.

Huppertz, T., Fox, P. F., & Kelly, A. L. (2018). The caseins: Structure, stability, and functionality. In Proteins in food processing (pp. 49-92). Woodhead Publishing.

Deng, L., Kang, X., Liu, Y., Feng, F., & Zhang, H. (2017). Effects of surfactants on the formation of gelatin nanofibres for controlled release of curcumin. Food chemistry, 231, 70-77.

Biranje, S., Madiwale, P., & Adivarekar, R. V. (2019). Porous electrospun Casein/PVA nanofibrous mat for its potential application as wound dressing material. Journal of Porous Materials, 26(1), 29-40.

Oroumei, A., Fox, B., & Naebe, M. (2015). Thermal and rheological characteristics of biobased carbon fiber precursor derived from low molecular weight organogold lignin. ACS Sustainable Chemistry & Engineering, 3(4), 758-769.

Foegeding, E. A., Davis, J. P., Doucet, D., & McGuffey, M. K. (2002). Advances in modifying and understanding whey protein functionality. Trends in Food Science & Technology, 13(5), 151-159.

Ramazani, S., Rostami, M., Raeisi, M., Tabibiazar, M., & Ghorbani, M. (2019). Fabrication of food-grade nanofibers of whey protein Isolate–Guar gum using the electrospinning method. Food Hydrocolloids, 90, 99-104.

Vega-Lugo, A. C., & Lim, L. T. (2012). Effects of poly (ethylene oxide) and pH on the electrospinning of whey protein isolate. Journal of Polymer Science Part B: Polymer Physics, 50(16), 1188-1197.

Matthews, J. A., Wnek, G. E., Simpson, D. G., & Bowlin, G. L. (2002). Electrospinning of collagen nanofibers. Biomacromolecules, 3(2), 232-238.

S. Sukigara, M. Gandhi, J. Ayutsede, M. Micklus, F. Ko, Regeneration of Bombyx mori silk by electrospinning—part 1: processing parameters and geometric properties, Polymer 44 (2003) 5721–5727

Adapa, S., Schmidt, K. A., & Toledo, R. (1997). Functional properties of skim milk processed with continuous high pressure throttling. Journal of Dairy Science, 80(9), 1941-1948.

Sullivan, S. T., Tang, C., Kennedy, A., Talwar, S., & Khan, S. A. (2014). Electrospinning and heat treatment of whey protein nanofibers. Food Hydrocolloids, 35, 36-50.

Tomasula, P. M., Sousa, A. M., Liou, S. C., Li, R., Bonnaillie, L. M., & Liu, L. (2016). Electrospinning of casein/pullulan blends for food-grade applications. Journal of dairy science, 99(3), 1837-1845.

Liu, J., Wang, Y., & Li, H. (2020). Synergistic solubilization of phenanthrene by mixed micelles composed of biosurfactants and a conventional non-ionic surfactant. Molecules, 25(18), 4327.

Gandhi, G., Amamcharla, J. K., & Boyle, D. (2017). Effect of milk protein concentrate (MPC80) quality on susceptibility to fouling during thermal processing. LWT-Food Science and Technology, 81, 170-179.

Deitzel, J. M., Kleinmeyer, J., Harris, D. E. A., & Tan, N. B. (2001). The effect of processing variables on the morphology of electrospun nanofibers and textiles. Polymer, 42(1), 261-272. Deitzel Deitzel

Appendix A

```
Data film;

input MCC $ PVA $ Vis Conductivity sur;
datalines;
8 1 8.4082 425 49.246
8 1 8.4971 425 49.246
8 1 8.9139 433 49.116
8 1 8.9139 433 49.256
8 1 7.9537 416 48.525
8 2 7.8943 416 49.057
8 2 25.343 468 49.284
8 2 25.415 468 49.36
8 2 29.188 478 48.412
8 2 25.918 478 49.133
8 2 27.674 458 49.17
8 2 24.939 458 49.36
8 3 70.266 489 49.057
8 3 72.171 489 49.578
8 3 70.602 496 49.888
8 3 73.644 496 49.603
8 3 88.321 502 49.74
8 3 83.914 502 49.664
10 1 11.666 483 49.578
10 1 11.227 483 49.057
10 1 12.463 467 49.17
10 1 12.382 467 49.019
10 1 11.064 479 49.398
10 1 11.395 479 49.778
10 2 40.787 516 49.019
```

10 2 40.357 516 48.146

10 2 41.149 519 49.246

10 2 40.341 519 49.36

10 2 39.832 512 49.892

10 2 40.292 512 49.93

10 3 121.35 531 50.515

10 3 122.27 531 50.433

10 3 129.4 531 50.273

10 3 124.7 531 49.778

10 3 125.15 534 50.501

10 3 123.67 534 50.311

12 1 18.925 534 49.019

12 1 19.307 534 49.17

12 1 21.811 532 49.854

12 1 22.297 532 50.006

12 1 20.012 502 49.968

12 1 20.474 502 50.082

12 2 77.498 574 49.892

12 2 78.705 574 49.93

12 2 65.235 554 51.225

12 2 66.681 554 49.93

12 2 76.899 550 50.844

12 2 71.179 550 50.577

12 3 188.3 560 50.806

12 3 191.65 560 50.691

12 3 185.4 548 51.187

12 3 187.62 548 50.577

12 3 197.56 562 50.806

12 3 198.21 562 51.225

14 1 37.853 555 49.095

14 1 33.871 555 49.246

```
14 1 28.622 550 49.133
14 1 29.507 550 49.095
14 1 32.16 545 49.133
14 1 31.359 545 48.791
14 2 88.63 583 49.74
14 2 92.469 583 49.892
14 2 96.797 572 49.892
14 2 102.11 572 49.778
14 2 90.437 552 49.436
14 2 92.911 552 49.512
14 3 313.72 576 51.148
14 3 318.25 576 51.225
14 3 378.79 568 52.14
14 3 382.49 568 51.835
14 3 378.79 566 52.14
14 3 382.49 566 51.835

run;

proc glimmix data = film;

            class MCC PVA;

            model Vis= MCC PVA MCC*PVA;

            lsmeans MCC*PVA / adjust=tukey lines;

run;

proc glimmix data = film;
```

```
            class MCC PVA;

            model Conductivity= MCC PVA MCC*PVA;

            lsmeans MCC*PVA / adjust=tukey lines;

run;

proc glimmix data = film;

            class MCC PVA;

            model sur=MCC PVA MCC*PVA;

            lsmeans MCC*PVA / adjust=tukey lines;

run;
```